molecules

MDPI

Article

Preparation of Naphthalene-Based Flame Retardant for High Fire Safety and Smoke Suppression of Epoxy Resin

Ziqin Huang [1], Fangli Li [1], Mingyan Huang [1], Wenqiao Meng [1], Wenhui Rao [1], Yuan Lei [2,*] and Chuanbai Yu [1,*]

[1] College of Materials Science and Engineering, Guilin University of Technology (GUT), Guilin 541004, China; 18776119751@163.com (Z.H.); 18579448271@163.com (F.L.); 18776030125@163.com (M.H.); mengwq@163.com (W.M.); raowh1@163.com (W.R.)

[2] China Antimony Corporation, Nanning 530001, China

* Correspondence: leiyuan2010@163.com (Y.L.); ycb2008@glut.edu.cn (C.Y.); Tel.: +86-189-7898-2120 (Y.L.); +86-133-9783-2021 (C.Y.)

Abstract: One of the current challenges in the development of flame retardants is the preparation of an environmentally friendly multi-element synergistic flame retardant to improve the flame retardancy, mechanical performance, and thermal performance of composites. This study synthesized an organic flame retardant (APH) using (3-aminopropyl) triethoxysilane (KH-550), 1,4-phthalaadehyde, 1,5-diaminonaphthalene, and 9,10-dihydro-9-oxa-10-phosphaphenanthrene-10-oxide (DOPO) as raw materials, through the Kabachnik-Fields reaction. Adding APH to epoxy resin (EP) composites could greatly improve their flame retardancy. For instance, UL-94 with 4 wt% APH/EP reached the V-0 rating and had an LOI as high as 31.2%. Additionally, the peak heat release rate (PHRR), average heat release rate (AvHRR), total heat release (THR), and total smoke produced (TSP) of 4% APH/EP were 34.1%, 31.8%, 15.2%, and 38.4% lower than EP, respectively. The addition of APH improved the mechanical performance and thermal performance of the composites. After adding 1% APH, the impact strength increased by 15.0%, which was attributed to the good compatibility between APH and EP. The TG and DSC analyses revealed that the APH/EP composites that incorporated rigid naphthalene ring groups had higher glass transition temperatures (Tg) and a higher amount of char residue (C_{700}). The pyrolysis products of APH/EP were systematically investigated, and the results revealed that flame retardancy of APH was realized by the condensed-phase mechanism. APH has good compatibility with EP, excellent thermal performance, enhanced mechanical performance and rational flame retardancy, and the combustion products of the as-prepared composites complied with the green and environmental protection standards which are also broadly applied in industry.

Keywords: epoxy resin; thermal performance; flame retardancy; smoke suppression

Citation: Huang, Z.; Li, F.; Huang, M.; Meng, W.; Rao, W.; Lei, Y.; Yu, C. Preparation of Naphthalene-Based Flame Retardant for High Fire Safety and Smoke Suppression of Epoxy Resin. *Molecules* **2023**, *28*, 4287. https://doi.org/10.3390/molecules28114287

Academic Editors: Lei Wang, Dong Wang and Keqing Zhou

Received: 10 May 2023
Revised: 18 May 2023
Accepted: 20 May 2023
Published: 24 May 2023

1. Introduction

Epoxy resin is an environmentally friendly thermosetting resin [1,2], which is widely used in electronic equipment, aerospace, national defense and the military industry and other industrial applications, due to its advantages of easy processing and good chemical stability [3,4]. Nevertheless, epoxy resin is an ignitable material that generates a lot of heat and smoke when burning, and hence is a considerable fire hazard, thereby limiting its application prospects [5–7].

In order to make it safer, the flame retardancy of the epoxy resin must be elevated using appropriate additives [8–11]. Based on the elements contained, flame retardants can be classified into halogen-free flame retardants and halogen-containing flame retardants [12,13]. Nevertheless, halogen-containing flame retardants produce a large quantity of toxic fumes when burned, which will cause harm to the environment and cause health issues. Hence, the focus of research has shifted to halogen-free flame retardants [14,15]. To improve flame retardancy, it is necessary to add a large amount of halogen-free flame retardants to the epoxy resin (e.g., aluminum hydroxide, aluminum phosphate, ammonium

polyphosphate) [16,17]. Nevertheless, halogen-free flame retardants often have disadvantages, such as large quantity requirements leading to a poor dispersion effect which affects the thermal or mechanical performance.

9,10-dihydro-9-oxa-10-phosphaphenanthrene-10-oxide (DOPO) is an environmentally friendly organic P flame retardant that has been widely applied in the production of flame-retarded epoxy resin [18–20]. However, the excellent flame retardancy of DOPO can only be achieved at high concentrations, while high DOPO content can lead to the drastic degradation of mechanical and thermal performance of flame-retarded epoxy resins [21]. To ensure a balanced performance, it is necessary to increase the reactive functional groups. Hence, the design and synthesis based on DOPO derivatives have attracted great attention. It is very challenging to combine P, N, and Si based on flame retardant synergies to create an environmentally friendly flame retardant that has a synergy with other properties. Li et al. [22] combined poly(vinyl)silazane (PVSZ) and DOPO through addition, to successfully prepare the phosphorus nitrogen silicon synergistic flame retardant (PPVSZ). When the PPVSZ content was 2.5 wt%, the UL-94 test reached the V-0 rating, the LOI reached 30%, and the impact strength increased by 45.38%, which significantly improved the flame retardancy and mechanical performance of epoxy resin. Unfortunately, this cannot preserve the thermal performance of composites. To improve the thermal performance, rigid groups, such as benzene ring, biphenyl ring, and naphthalene ring, can be introduced into the system to increase the rigidity of the molecular segments and effectively improve the thermal resistance of the epoxy resin curing system [23–25]. Gao et al. [26] synthesized the bio-based epoxy monomer diglycidyl ether luteolin (DGEL) from luteolin. The test results showed that the Tg of DGEL/DDS reached 314.4 °C, and the vertical burning test (UL-94) reached the V-0 level, which has both good flame retardancy and good thermal performance. This is because the aromatic rings and multifunctional groups in luteolin improve the thermal stability. By designing novel epoxy resin molecular chains, compounds with rigid groups can be used as monomers to synthesize novel epoxy resin prepolymers and improve the thermal stability of polymers. Although the excellent effect can be obtained in this way, the operation is complicated and it is not amenable to large-scale production. Therefore, realizing excellent mechanical performance, thermal performance, and flame retardancy of phosphazidosilane compounds in EP composites based on the multi-component synergistic effect is a priority [27–29].

In this study, a novel P-containing nitrogen silane compound was synthesized; a novel flame retardant, APH, was synthesized by using DOPO, KH550, 1,5-diaminonaphthalene, and terephthalaldehyde via the Kabachnik-Fields reaction. In addition, the quantity of APH added and its effect on the mechanical performance, thermal performance, and flame retardancy of EP composites were analyzed. Analysis of the structure and morphology of products in the thermal decomposition of APH/EP composites, components, and carbon residue revealed the mechanism of flame retardancy of APH in the combustion process.

2. Results and Discussion

2.1. Material Characterization of APH

The synthetic route of APH is shown in Scheme 1. The flame retardant APH was synthesized via the Kabachnik-Fields reaction of KH-550, 1,4-phthalaadehyde, 1,5-diaminonaphthalene, and DOPO. The abundant active amines in APH could participate in the curing reaction of EP, thereby improving the interface compatibility between the flame retardant and EP matrix. Additionally, the introduced naphthalene ring structure could improve the mechanical and thermal performances of the composites. The P–N–Si elements in APH could achieve a synergistic flame-retardant effect, thus endowing the APH/EP composite with high flame retardancy.

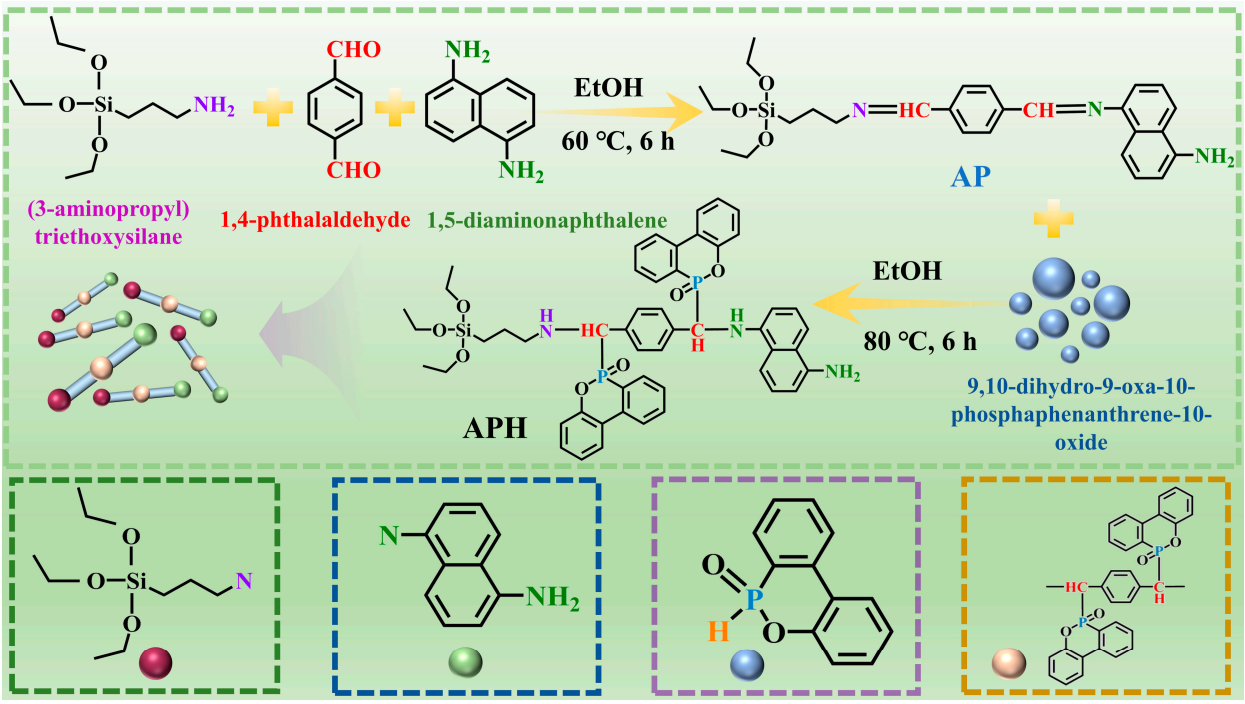

Scheme 1. Synthetic route of APH.

Figure 1a showed the FT-IR spectra of APH. As observed, the absorption peak at 2389 cm^{-1} on DOPO corresponds to P-H, the absorption peak of 1695 cm^{-1} on terephthalaldehyde corresponds to C=O, and the characteristic peak at 3376 cm^{-1} on 1,5-diaminonaphthalene is attributed to the N-H stretching vibration of the primary amino group [30]. It was observed that the peak at 2389 cm^{-1} on DOPO and the peak at 1695 cm^{-1} on terephthalaldehyde disappeared at APH, and the double band at 3376 cm^{-1} in 1,5-diaminonaphthalene became a single broad resolution in the APH band [31]. The center was at 3400 cm^{-1} and the absorption peaks of the P–C and P–O–C bonds were at 760 cm^{-1} and 1203 cm^{-1} of APH, respectively, suggesting that aminomethylation occurred during the reaction [32,33]. Figure 1b showed the SEM images of APH. As observed, the APH granule grew with a mushroom structure. Figure 1c,d showed the ^{1}H NMR spectrum and ^{31}P NMR spectrum of APH. The attribution of each peak in the relevant ^{1}H NMR is as follows: δ = 0.33 ppm (q, 2H, –Si–CH_2–CH_2–), (labeled "c"), 1.1 ppm (q, 2H, CH_3–CH_2–O–Si–), (labeled "a"), 1.22 ppm (q, 2H, –CH_3–CH_2–CH_2–), (labeled "d"), 2.49 ppm (q, 2H, –NH_2–), (labeled "e"), 3.4 ppm (q, 2H, –CH_2–CH_2–NH–), (labeled "f"), 4.35 ppm (q, 2H, CH_3–CH_2–O–Si–), (labeled "b"), 7–8 ppm (m, Ar–H), (labeled "h"), 8.26 ppm (d, 1H, CH), (labeled "g"). ^{31}P NMR (DMSO-d_6, 400 MHz): δ = 33.5 ppm.

From the above data, the peaks in the range of 8.4–7.0 ppm on the APH in the ^{1}H NMR spectrum correspond to the hydrogen signals on the benzene ring. A single peak appeared at 33.5 ppm in the ^{31}P NMR spectrum, while the ^{31}P NMR spectrum peak of DOPO was located at 13–17 ppm [34]. The combination of FT-TR and NMR results indicated the successful synthesis of APH.

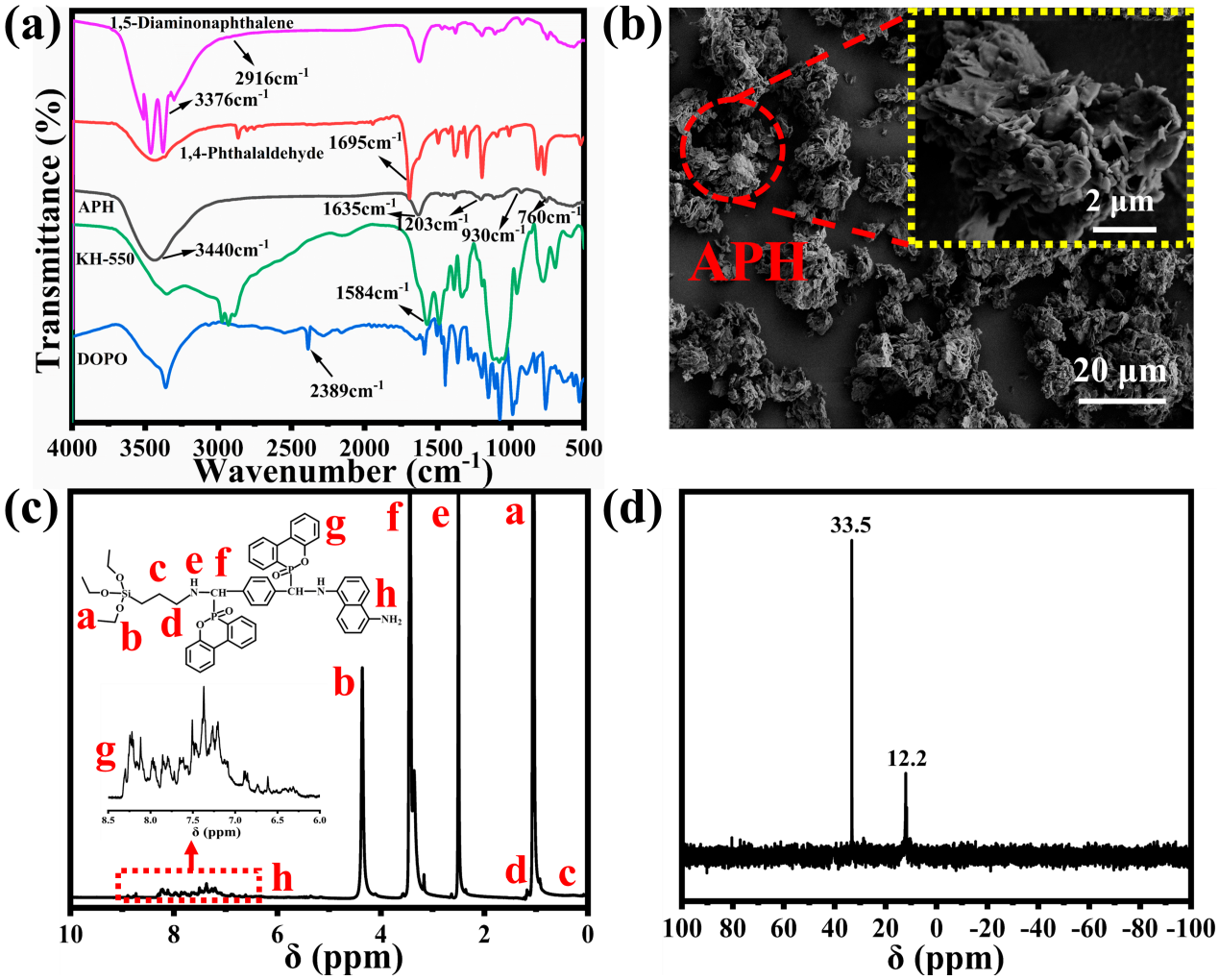

Figure 1. FT-IR spectra of 1,5-diaminonaphthalene, 1,4-phthalaadehyde, KH-550, DOPO and APH (**a**); SEM images of APH (**b**); ^{1}H NMR spectra (**c**) and ^{31}P NMR spectra (**d**) of APH.

2.2. Flame Retardancy

The UL-94 and LOI tests were applied on EP and APH/EP to evaluate the flame retardancy of composites in air. According to Figure 2a,b,d,e and Table 1, the LOI of EP was 23.3%, and the total ignition time (TTI) was 80 s. It did not pass the UL-94 test level, suggesting that EP was flammable in air, and there was a fire safety hazard [35]. As a comparison, after adding the flame retardant, the vertical burning time was shortened and the limiting oxygen index was increased. The LOI of 4% APH/EP was as high as 31.2%, and it reached the V-0 grade, suggesting that the addition of APH markedly improved the flame retardancy of the composites.

Table 1. UL-94 test results and LOI of EP and flame-retardant EP.

Sample	t_1/t_2 (s)	Rating	Dripping (Yes/No)	LOI (%)
EP	192/0	Fail to pass	No	23.5
1% APH/EP	13/12	V-1	No	29.8
2% APH/EP	10/4	V-1	No	30.7
3% APH/EP	4/6	V-0	No	30.9
4% APH/EP	3/4	V-0	No	31.2

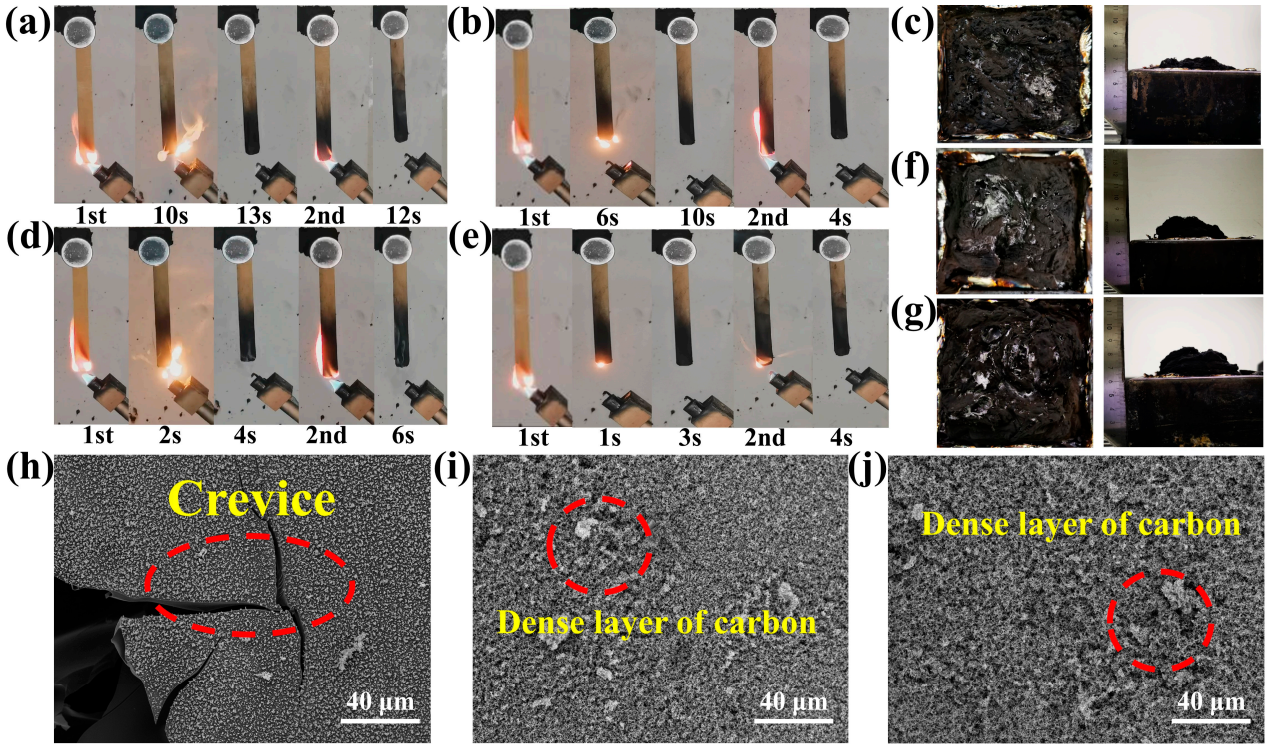

Figure 2. UL-94 images of 1% APH/EP (**a**), 2% APH/EP (**b**), 3% APH/EP (**d**) and 4% APH/EP (**e**); EP (**c**), 2% APH/EP (**f**) and 4% APH/EP (**g**) carbon residue images after CC test; SEM images of carbon residue of EP (**h**), 2% APH/EP (**i**) and 4% APH/EP (**j**) after CC test.

Cone calorimeter tests are used to appraise the combustion properties of the polymer. Several key parameters can be obtained through cone calorimetry, for instance, the heat release rate (HRR), smoke release rate (SPR), total heat release (THR), CO production (COP), and total smoke produced (TSP) [36]. The time-varying trends of the above parameters for pure EP and composites containing 2 wt% and 4 wt% APH are displayed in Figure 3a–e, respectively. The relevant data are summarized in Table 2. The PHRR, TSP, and THR of pure EP were as high as 1383.6 kW/m^2, 61.0 m^2, and 79.0 MJ/m^2, respectively, indicating that the combustion ability of EP was very strong [37]. As a comparison, the PHRR of 2% APH/EP and 4% APH/EP was 877.3 and 912.1 kW/m^2, respectively, which were 36.6% and 34.0% lower than EP, and the TSP and THR were also significantly lower than pure EP. This can be assigned to the fact that APH released a large quantity of P-containing free radicals during the combustion process, captured the free radicals produced, and inhibited the combustion process, suggesting that the addition of APH can effectively reduce the combustion ability of composites. As shown in Figure 3b, the SPR exhibited the same trend as the HRR. Among them, the SPR peak of 4% APH/EP was significantly lower than that of EP. This was probably attributed to the enhanced structural stability of the residual char in the epoxy composites. The dense residual char layer could isolate heat and combustible gases, and reduced the SPR. The percentage of carbon residue (W_{700}) increased from 11.8% to 19.4%. This was due to the accumulation of phosphoric acid derivatives generated by APH on the surface of the composites during combustion, promoting the formation of carbon residue and effectively blocking the exchange of heat and volatiles [38]. The increase in the carbon residue content showed that APH has better condensed-phase flame retardancy.

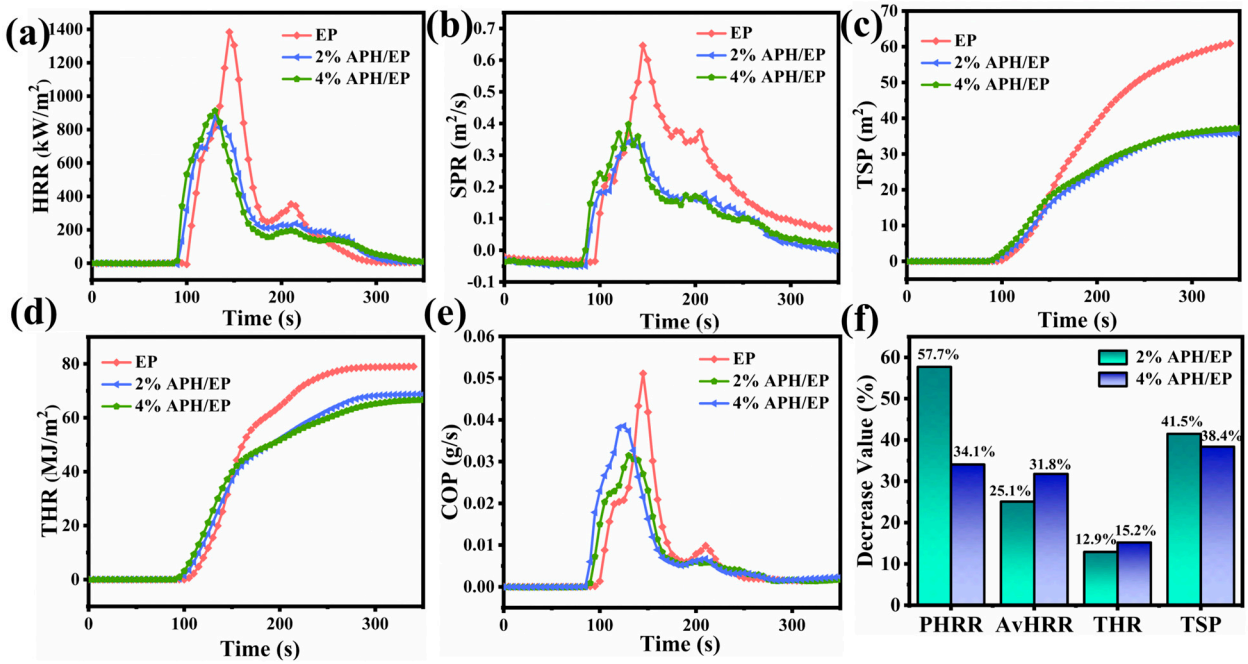

Figure 3. HRR (**a**), SPR (**b**), TSP (**c**), THR (**d**), COP (**e**) curves and reduction values (**f**) for EP, 2% APH/EP and 4% APH/EP.

Table 2. Cone calorimetric data of EP and flame-retardant EP.

Sample	EP	2% APH/EP	4% APH/EP
PHRR (kW/m^2)	1383.6	877.3	912.1
av-HRR (kW/m^2)	322.2	241.4	219.8
TSP (m^2)	61.0	35.7	37.6
THR (MJ/m^2)	79.0	68.8	67.0
COP (g/s)	0.052	0.031	0.038
Char residue (wt%)	11.8	15.2	19.4

Figure 3e was the COP curve of EP and its composites, and the specific trend was the same as that of HRR and SPR. As depicted in Figure 3e, the COP of EP was 0.051 g/s, and the COP corresponding to the addition of 2 wt% and 4 wt% APH was 0.032 and 0.038 g/s, respectively, which was 37.2% and 25.5% lower than that of pure EP. This can be attributed to the fact that APH forms a dense char layer during combustion, which acts as a physical barrier and prevents the combustible gas from escaping.

Figure 2c,f,g show EP, 2% APH/EP, and 4% APH/EP carbon residue images after the CC test, and Figure 2h–j are their corresponding SEM images. According to Figure 2c, the carbon residue surface of EP was relatively broken, the expansion range was small, and the corresponding SEM images have obvious cracks. According to Figure 2f,g, the surface of the carbon residue after adding APH was relatively complete, firm, and swollen, and combined with SEM diagrams, it can be seen that the addition of APH resulted in the formation of a dense carbon layer on the composites. The above data demonstrated that the addition of APH could effectively enhance the flame retardancy of composites.

2.3. Mechanism of Flame Retardancy

Raman spectroscopy and XPS were used to clarify the mechanism of flame retardancy. Figure 4a–c show the Raman spectra of the char residue after the CC tests of EP, 2% APH/EP, and 4% APH/EP samples, respectively. The D band (1343 cm^{-1}) and G band (1585 cm^{-1}) represent the absorption peaks of disordered carbon and sp_2 hybridized carbon atoms, respectively [39]. Meanwhile, the carbon residues after combustion were assessed on the basis of the I_D/I_G ratio, which reflects the degree of orderliness in the carbon atoms, to

clarify the graphitization level. As shown in Figure 4a, the I_D/I_G ratio of EP was the highest (3.1), while the I_D/I_G ratios of 2% APH/EP and 4% APH/EP were 2.8 and 2.7, respectively, which were lower than those of pure EP. The Raman spectrum indicated that APH can promote the formation of the carbon residue, which is beneficial to enhancing the flame retardancy of the composites [40].

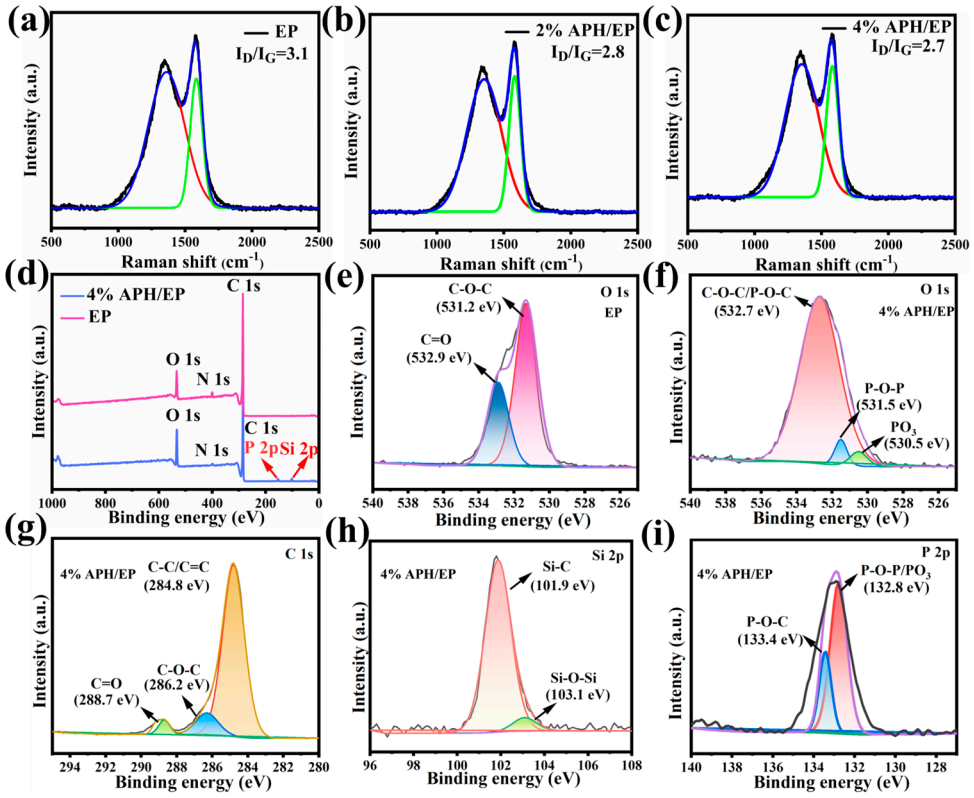

Figure 4. Raman test curves of char residual for EP (**a**), 2% APH/EP (**b**) and 4% APH/EP (**c**) after CC test; full XPS spectrums (**d**), O 1s spectrums of char residual for EP after CC test (**e**), O 1s spectrum of char residual for 4% APH/EP after CC test (**f**), C 1s spectrums (**g**), Si 2p spectrums (**h**) and P 2p spectrums (**i**) of char residual for 4% APH/EP after CC test.

Figure 4d was the XPS full spectrum of carbon residue of 4% APH/EP after the CC test, and the specific composition is shown in Table 3. Figure 4f–i are the O 1s, C 1s, Si 2p, and P 2p spectrums of the carbon residue of 4% APH/EP after the CC test. As indicated by the C 1s spectrum (Figure 4g), the peaks at 286.2 and 288.7 eV belong to the C–O–C bonds and C=O bonds, while the C–C bonds and C=C bonds of the multi-aromatic structures have a peak at 284.8 eV, suggesting that carbon was mainly in the oxidized state at medium and low temperatures. As indicated by the O 1s spectra (Figure 4f), the peaks at 530.5 eV, 531.5 eV, and 532.7 eV were ascribed to PO_3, P–O–P, and C–O–C/P–O–C, respectively. By comparing the O 1s curves of residual char with the 4% APH/EP composite material (Figure 4f), it was found that the O 1s curves of pure EP (Figure 4e) did not contain phosphorus elements. As indicated by the Si 2p spectrum (Figure 4h), Si–C and Si–O–Si have peaks at 101.9 and 103.1 eV, respectively [41]. As indicated by the P 2p spectrum (Figure 4i), the peaks at 132.8 and 133.4 eV belong to P–O–P/PO_3 and P–O–C [42]. The above results indicate that APH would generate polyphosphate during the combustion process, facilitate the formation of a dense coke layer, isolate the combustible gas, and exhibit a condensed state mechanism of flame retardancy.

Table 3. Relative element content of the char residue of 4% APH/EP.

Sample	C (wt%)	O (wt%)	N (wt%)	P (wt%)	Si (wt%)
4% APH/EP	81.41	13.04	4.30	0.53	0.72

The TG-FTIR test was applied to characterize the combustibles, and the gaseous products released during the combustion of EP were analyzed. Figure 5c,d. showed the FT-IR spectra of the thermal degradation products of EP and APH/EP. As observed, the characteristic peak of the epoxy resin and its composites under different degradation temperatures was basically the same [43]. The absorption peak of water or hydroxyl was located at 3650 cm^{-1}; 2900 cm^{-1} corresponds to hydrocarbons, 2350 cm^{-1} corresponds to carbon dioxide, 1710 cm^{-1} represents carbonyl compounds, and aromatic compounds and ethers are at 1520 cm^{-1} and 1150 cm^{-1}, respectively [44,45]. As shown in Figure 5d, 4% APH/EP has a characteristic absorption peak of higher intensity in the vicinity of 350 °C, which can be attributed to the degradation of phosphorus oxides in APH. Figure 5e–j show the relationship between the absorption intensity and time of volatiles during the thermal degradation of EP and 4% APH/EP. As observed, after the addition of APH the amount of combustible gas in the thermal degradation of the material dropped drastically. As shown in Figure 5a,b, the difference in gaseous pyrolysis products released by EP and 4% APH/EP were not significant, and Figure 5e displays the fact that the absorption peak of water or hydroxyl is significantly enhanced, suggesting that the flame-retardant process produces more moisture [46]. In combination with the laboratory results of CC, this suggests that it may be caused by the dehydration of APH into carbon. Compared with EP, the intensities of other characteristic peaks were all lower, indicating that the addition of APH reduced the release of organic volatiles such as carbonyl compounds and aromatic compounds in EP composites without significantly changing the gaseous volatiles of composites, so that the APH/EP composite has better flame retardancy and smoke suppression capability [47].

The conception of the principle is shown in Scheme 2, which explains the mechanism of the addition of APH to enhance the flame retardancy of EP composites. The synergistic effect of P/N/Si in APH could accelerate the formation of carbon residue. Under the synergistic effect of the P/N/Si compounds, the dense carbon layer formed during APH combustion acted as a physical barrier that could isolate the penetration of oxygen and combustible gas and reduced heat release at the same time, which was mainly manifested in the condensed-phase mechanism of flame retardancy.

2.4. Thermal Stability

The thermal stability of epoxy resin-cured products under N_2 was investigated. Figure 6a shows the TG curves of pure EP and EP with 2 wt% and 4 wt% APH. As shown in Figure 6a, the cured products of the epoxy resin all exhibited a one-step decomposition process. As depicted in Figure 6b, the weight-loss range of the epoxy cured product was from 360 °C to 460 °C, and the amount of carbon residue increased progressively with the increase in the mass of APH. Table 4 summarizes the maximum degradation temperature (T_{max}), the initial degradation temperature ($T_{5\%}$), maximum mass loss rate (R_{Tmax}), and carbon residue (C_{700}) of composites at 700 °C. As depicted in Table 4, $T_{5\%}$, T_{max}, R_{Tmax} all decreased with the increase in APH mass. $T_{5\%}$ decreased from 399.4 °C to 389.4 °C. This can be assigned to the fact that during the early decomposition of APH it decomposes into phosphoric acid compounds at high temperature, with poor stability [48]. R_{Tmax} decreased from 1.8%/°C to 1.4%/°C, suggesting that the addition of APH reduced the combustion decomposition rate of the composites and promoted the generation of a coke layer. C_{700} increased from 19.5% to 22.0%, as APH/EP produced a variety of phosphoric acid substances during the decomposition process, which promoted the increase in carbon residue.

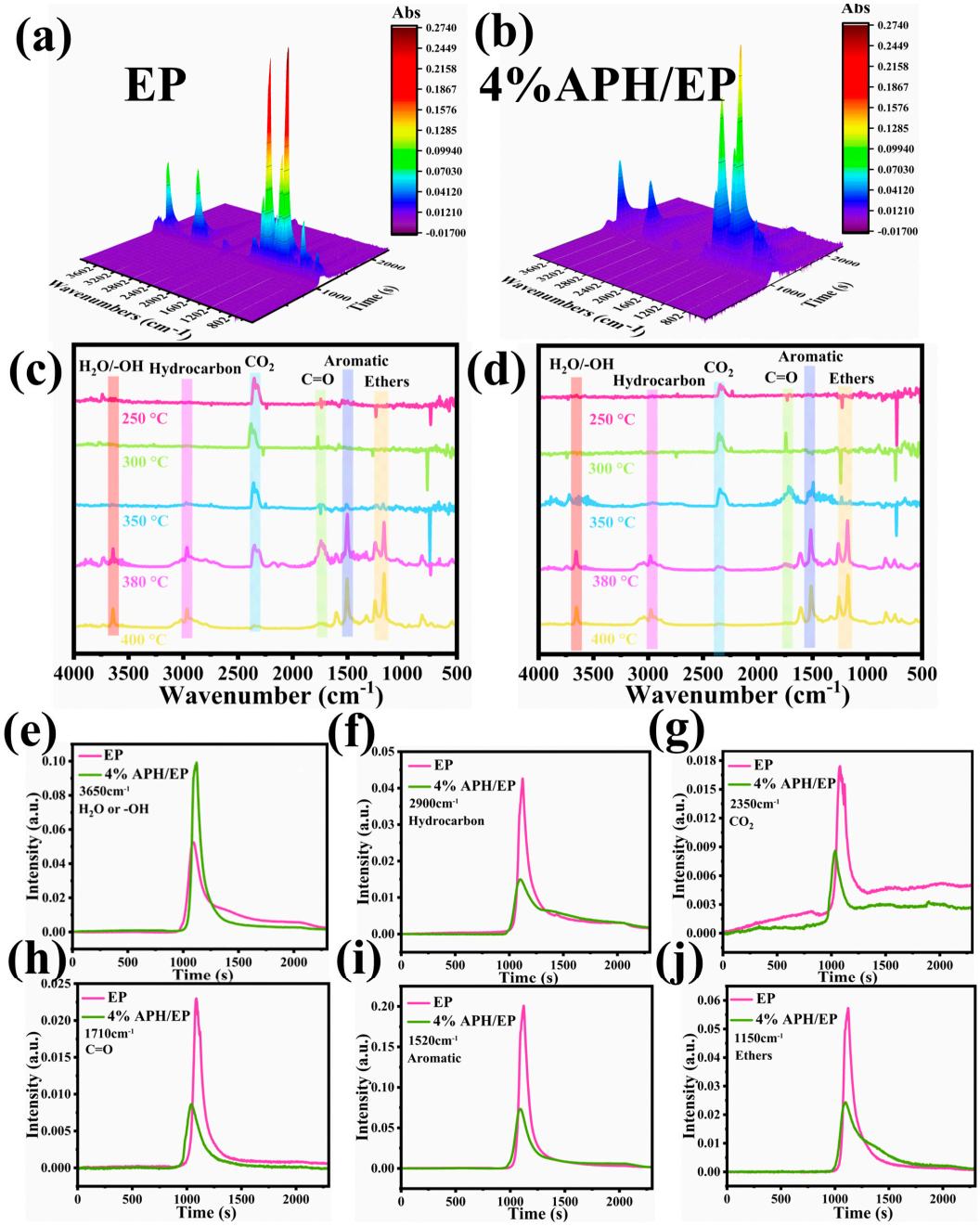

Figure 5. TG-FTIR test 3D spectrums of EP (**a**) and 4% APH/EP (**b**); FTIR spectrums of EP (**c**) and 4% APH/EP (**d**); absorption intensity versus time for EP and 4% APH/EP (**e**–**j**) volatiles during thermal degradation.

Table 4. Concrete TGA data of EP, 2% APH/EP and 4% APH/EP.

Sample	$T_{5\%}$ (°C)	T_{max} (°C)	R_{Tmax} (%/°C)	C_{700} (wt%)
EP	399.4	419.1	1.8	19.5
2% APH/EP	390.4	415.2	1.5	20.1
4% APH/EP	389.4	414.2	1.4	22.0

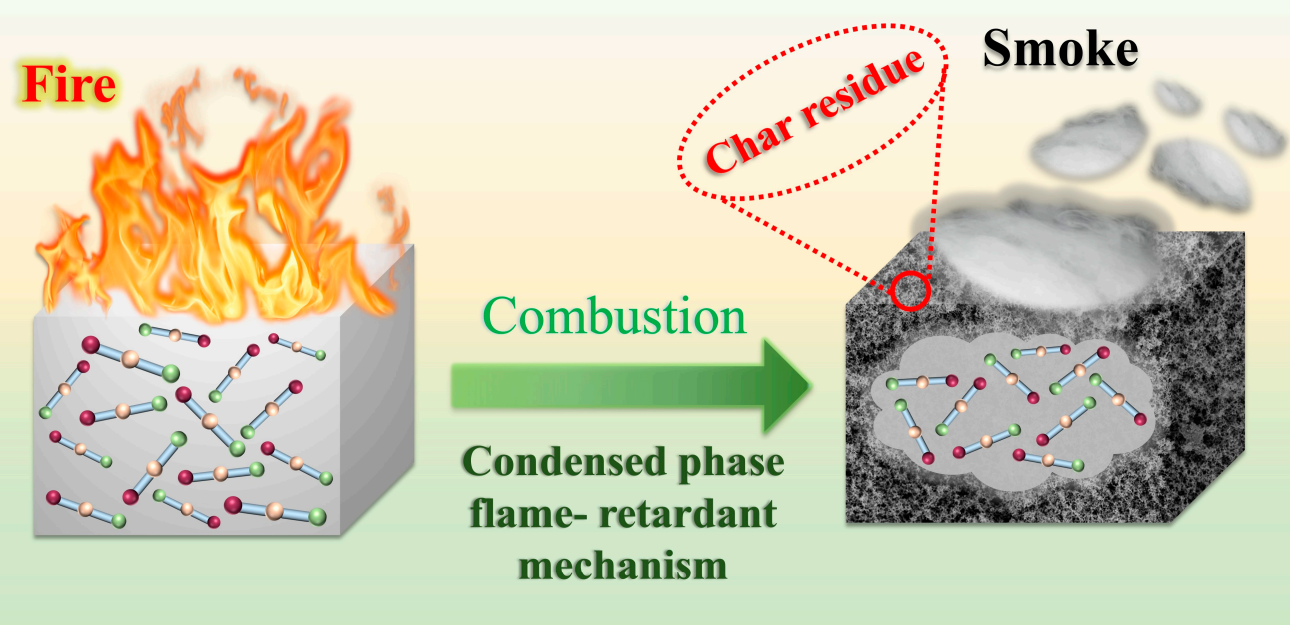

Scheme 2. Mechanism of flame retardancy of APH in EP.

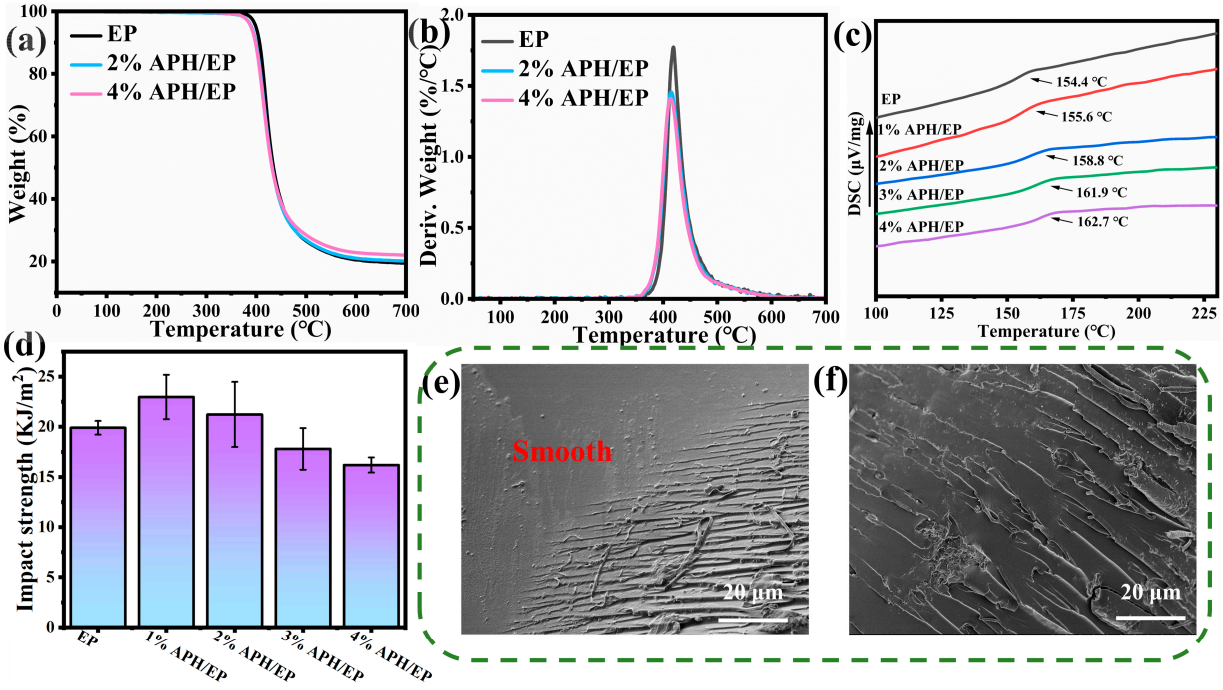

Figure 6. TG curves of EP and flame-retarded EP (**a**); DTG curves of EP and flame-retarded EP (**b**); DSC curves of EP and flame-retarded EP (**c**); impact strength (**d**) of EP and flame-retarded EP, (**e**) and SEM images of impact section of 1% APH/EP (**f**).

The thermal performance of the composites was further explored by using the DSC test. Figure 6c shows the DSC curves of the EP and APH/EP composites. As observed, the glass transition temperature (Tg) of pure EP was 154.4 °C, and when the added APH was 1 wt%, 2 wt%, 3 wt%, and 4 wt%, the glass transition temperature became 155.6 °C, 158.8 °C, 161.9 °C, and 162.7 °C, respectively. The Tg of the composites increased as the amount of added flame retardant increased. This may be because the rigid naphthalene ring groups introduced in APH can increase the rigidity of the molecular chain segment

and the compactness of the cross-linked network after the epoxy resin was cured, thus leading to the improvement in the APH/EP composite thermal resistance [49].

2.5. Mechanical Performance

Epoxy resin is a commonly used thermosetting resin, and modification for flame retardancy should consider its mechanical performance, especially toughness. Figure 6d shows the impact strength diagram of EP and APH/EP composites. As observed, the impact strength of pure EP was 20 KJ/m^2; when the added amount was 1 wt%, the impact strength rose to 23 KJ/m^2, which was 15% higher than that of pure EP. As the amount of added APH increased, the impact strength decreased gradually. When the added amount was 3 wt%, the impact strength dropped to 17.88 KJ/m^2, which was lower than that of pure EP. This can be assigned to the fact that APH contains many rigid groups, and when the proportion increases the flame-retardant agglomerates in EP, resulting in a decline in the mechanical performance. Figure 6e,f are the SEM images of the impact sections of EP and 1% APH/EP. According to Figure 6e, the impact section of EP is smooth, with flat lines, showing brittle fracture characteristics. According to Figure 6f, the impact section of 1% APH/EP shows wrinkles without agglomeration, and the appearance of these wrinkles effectively disperses the impact force, which is beneficial to the improvement of impact strength.

3. Experimental

3.1. Materials

Ethanol, 1,4-phthalaadehyde, 1,5-diaminonaphthalene and 3-aminopropyltriethoxysilane (KH550, AR, 98%) were purchased from Sichuan Xilong Science Co., Ltd. (Chengdu, China). Epoxy resin (E51, epoxy value = 0.51) was purchased from Sinopec (Beijing, China). 4,4-Diaminodiphenylmethane (DDM) was purchased from Sichuan Xilong Science Co., Ltd. (Chengdu, China). DOPO was acquired from Guangdong Wengjiang Co., Ltd. (Shaoguan, China). Further purification was not applied for any purchased reagent.

3.2. Synthesis of Flame Retardant APH

Firstly, 5.2733 g of 1,5-diaminonaphthalene and 14.5799 g of KH-550 were weighed and added into a 500 mL three-necked flask, and 50 mL of ethanol was added as solvent. The solution was then ultrasonicated for 10 min; 13.4132 g of 1,4-phthalaadehyde was dissolved in 50 mL of ethanol, followed by addition to the as-prepared system. The temperature was set to 60 °C, and the product was condensed and refluxed with magnetic stirring for 5 h. Subsequently, 30.0000 g of DOPO was dissolved in 100 mL of ethanol and the DOPO solution was added to the product. The temperature was raised to 80 °C and maintained for 6 h. After cooling down to room temperature, the solution was filtered and the product was rinsed with ethanol, dried under vacuum at 60 °C for 24 h, ground, and sieved for later use. The product so obtained was denoted as APH.

3.3. Preparation of EP and APH/EP Composite

EP (E51) was preheated at 60 °C for half an hour and flame retardant APH and EP were mixed and magnetically stirred at 80 °C for 1 h to obtain a uniformly dispersed mixture. After mixing evenly, the melted curing agent DDM was added and subjected to vacuum until no bubbles were released. Then, the mixture was added to the preheated mold and cured at 80 °C/2 h, 100 °C/2 h, and 130 °C/2 h. The mass of APH was 1 wt%, 2 wt%, 3 wt%, 4 wt%, and 5 wt%, respectively. The ratio of different EP composites is shown in Table 5.

Table 5. Specific proportions of epoxy composites.

Sample	EP (g)	DDM (g)	APH (g)
EP	80.00	20.00	0.00
1% APH/EP	80.00	20.00	1.01
2% APH/EP	80.00	20.00	2.04
3% APH/EP	80.00	20.00	3.09
4% APH/EP	80.00	20.00	4.16

3.4. Test Characterization

Characterization using Fourier-transform infrared (FT-IR) spectroscopy (NEXUS 6700 FT-IR spectrometer, Thermo Nicolet, Waltham, MA, USA, wavenumber = 500–4000 cm^{-1}), X-ray photoelectron spectroscopy (ESCALAB 250Xi, Thermo Fisher Scientific, MA, USA, 1361 eV Al Ka), scanning electron microscopy (SEM) (S-4800H, Japanese High tech Company, Tokyo, Japan), NMR spectroscopy (^{1}H and ^{31}P, Bruker AV 400, German company, Karlsruhe, Germany, with deuterated DMSO-d_6 as the solvent), and TGA (TA Q500, TA Company, Newcastle, DE, USA, 35–700 °C under N_2, 10 °C min^{-1}) were applied to the samples. Additionally, the limiting oxygen indexes (LOI) (JF-3, China Jiangning Analytical Instrument Co., Ltd., Nanjing, China) of the samples were obtained, wherein the sample had a size of 130.0 × 6.5 × 3.2 mm^3.

The UL-94 vertical burning test (YK-3050, Dongguan Youke Equipment Co., Ltd., Dongguan, China) was executed on samples with sizes of 130.0 × 13.0 × 3.2 mm^3. A cone calorimeter test (MC-3001, FTT Company, East Grinstead, UK, radiation intensity = 35 kW/m^2) was executed to clarify the combustion behaviors, wherein the sample had a size of 100 × 100 × 3 mm^3. Raman spectroscopy (DXR, American Thermal Power Company, Milford, MA, USA, 10 s, excitation wavelength = 532.17 nm) was applied to the samples. The unnotched impact test (DR-802B, SANS Company, Shenzhen, China) was executed on samples with a size of 80 × 10 × 4 mm^3. TG-FTIR (NEZTSCH STA 449 F, Shanghai Fairborn Precision Instrument Co., Ltd., Shanghai, China) tests were also conducted.

4. Conclusions

To popularize epoxy resin composites, it is very important to consider both mechanical performance and thermal properties during flame retardancy modification. In this work, a flame retardant APH was designed and synthesized. When the addition of APH was 1 wt%, the impact strength increased by 15.0%, in contrast to that of pure EP. Meanwhile, the rigid groups in APH were beneficial to the maintenance of thermal stability. Analysis of the flame-retarding performance indicated that 4% APH/EP could pass the V-0 grade of vertical combustion, and its LOI could reach 31.2%. Compared with pure EP, the PHRR, THR, and TSP of 4% APH/EP decreased by 34.1%, 15.2%, and 38.4%, respectively. In addition, the presence of APH reduced toxic gas (CO) emissions by 25.5%, and increased carbon residues. Compared with pure EP, the APH/EP composite had excellent mechanical performance, good thermal stability and flame retardancy, and rational smoke suppression. Furthermore, the P/N/Si compounds in APH showed a good synergistic effect, and the dense carbon layer formed during the combustion process served as a physical barrier that could effectively reduce the heat release and combustible gas emissions, mainly exhibiting a condensed-phase flame-retardant mechanism. This study provided a broad prospect for the fire safety application of epoxy resin composites.

Author Contributions: Methodology, writing, and editing, Z.H.; investigation and validation, F.L.; data curation and material characterization, M.H.; idea and investigation, W.M.; writing—original draft, Writing—review & editing, W.R.; conceptualization, investigation, writing-review & editing, Y.L.; resources, funding acquisition, supervision, writing, and editing, C.Y. All authors have read and agreed to the published version of the manuscript.

Funding: This study was funded by the National Natural Science Foundation of China (Grant No: 51563004), Natural Science Foundation of Guangxi Province (2022GXNSFAA035566), Foundation of Guilin University of Technology (GLUTQD2002029) and Nanning Science and Technology Planning Project (20221035).

Institutional Review Board Statement: Not applicable.

Informed Consent Statement: Not applicable.

Data Availability Statement: The data presented in this study are available in this manuscript.

Conflicts of Interest: The authors declare no conflict of interest.

Sample Availability: Not applicable.

References

1. Zhang, J.; Mi, X.; Chen, S.; Xu, Z.; Zhang, D.; Miao, M.; Wang, J. A bio-based hyperbranched flame retardant for epoxy resins. *Chem. Eng. J.* **2020**, *381*, 122719. [CrossRef]
2. Zhong, L.; Hao, Y.; Zhang, J.; Wei, F.; Li, T.; Miao, M.; Zhang, D. Closed-loop recyclable fully bio-based epoxy vitrimers from ferulic acid-derived hyperbranched epoxy resin. *Macromolecules* **2022**, *55*, 595–607. [CrossRef]
3. Tian, Y.; Wang, Q.; Shen, L.; Cui, Z.; Kou, L.; Cheng, J.; Zhang, J. A renewable resveratrol-based epoxy resin with high Tg, excellent mechanical properties and low flammability. *Chem. Eng. J.* **2020**, *383*, 123124. [CrossRef]
4. Kandola, B.K.; Magnoni, F.; Ebdon, J.R. Flame retardants for epoxy resins: Application-related challenges and solutions. *J. Vinyl. Addit. Technol.* **2022**, *28*, 17–49. [CrossRef]
5. He, L.X.; Liu, X.D.; Zheng, X.T.; Dong, Y.Q.; Bai, W.B.; Lin, Y.C.; Jian, R.K. A versatile phosphorothioate bearing benzimidazole for the preparation of flame retardant, mechanically strong and high transparency epoxy resins. *Polym. Degrad. Stab.* **2022**, *203*, 110056. [CrossRef]
6. Jian, R.K.; Pang, F.Q.; Lin, Y.C.; Bai, W.B. Facile construction of lamellar-like phosphorus-based triazole-zinc complex for high-performance epoxy resins. *J. Colloid Interface Sci.* **2022**, *609*, 513–522. [CrossRef]
7. Liu, X.D.; Zheng, X.T.; Dong, Y.Q.; He, L.X.; Chen, F.; Bai, W.B.; Lin, Y.C.; Jian, R.K. A novel nitrogen-rich phosphinic amide towards flame-retardant, smoke suppression and mechanically strengthened epoxy resins. *Polym. Degrad. Stab.* **2022**, *196*, 109840. [CrossRef]
8. Chu, F.; Hu, W.; Song, L.; Hu, Y. State-of-the-art research in flame-retardant unsaturated polyester resins: Progress, challenges and prospects. *Fire Technol.* **2022**, 1–42. [CrossRef]
9. Wang, L.; Wei, Y.; Deng, H.; Lyu, R.; Zhu, J.; Yang, Y. Synergistic flame retardant effect of barium phytate and intumescent flame retardant for epoxy resin. *Polymers* **2021**, *13*, 2900. [CrossRef]
10. Zhao, S.; Chen, X.; Zhou, Y.; Zhao, B.; Hu, Q.; Chen, S.; Pan, K. Molecular design of reactive flame retardant for preparing biobased flame retardant polyamide 56. *Polym. Degrad. Stab.* **2023**, *207*, 110212. [CrossRef]
11. Bekeshev, A.; Mostovoy, A.; Shcherbakov, A.; Zhumabekova, A.; Serikbayeva, G.; Vikulova, M.; Svitkina, V. Effect of phosphorus and chlorine containing plasticizers on the physicochemical and mechanical properties of epoxy composites. *J. Compos. Sci.* **2023**, *7*, 178. [CrossRef]
12. Wang, C.; Zhang, Y.; Wang, X. Preparation and properties of epoxy resin modified with phosphorus and nitrogen flame retardants. *Mater. Res. Express* **2023**, *10*, 035303. [CrossRef]
13. Li, G.; Wang, W.; Cao, S.; Cao, Y.; Wang, J. Reactive, intumescent, halogen-free flame retardant for polypropylene. *J. Appl. Polym. Sci.* **2014**, *131*, 40054. [CrossRef]
14. Lampa, E.; Eguchi, A.; Todaka, E.; Mori, C. Fetal exposure markers of dioxins and dioxin-like PCBs. *Environ. Sci. Pollut. Res. Int.* **2018**, *25*, 11940–11947. [CrossRef] [PubMed]
15. Zhang, M.; Buekens, A.; Li, X. Open burning as a source of dioxins. *Crit. Rev. Environ. Sci. Technol.* **2017**, *47*, 543–620. [CrossRef]
16. Huang, Z.; Ruan, B.; Wu, J.; Ma, N.; Jiang, T.; Tsai, F.C. Highefficiency ammonium polyphosphate intumescent encapsulated polypropylene flame retardant. *J. Appl. Polym. Sci.* **2020**, *138*, 50413. [CrossRef]
17. Chai, G.; Zhu, G.; Gao, S.; Zhou, J.; Gao, Y.; Wang, Y. On improving flame retardant and smoke suppression efficiency of epoxy resin doped with aluminum tri-hydroxide. *Adv. Compos. Lett.* **2019**, *28*, 19894597. [CrossRef]
18. Chi, Z.; Guo, Z.; Xu, Z.; Zhang, M.; Li, M.; Shang, L.; Ao, Y. A DOPO-based phosphorus-nitrogen flame retardant bio-based epoxy resin from diphenolic acid: Synthesis, flame-retardant behavior and mechanism. *Polym. Degrad. Stab.* **2020**, *176*, 109151. [CrossRef]
19. Yang, Y.; Wang, D.Y.; Jian, R.K.; Liu, Z.; Huang, G. Chemical structure construction of DOPO-containing compounds for flame retardancy of epoxy resin: A review. *Prog. Org. Coat.* **2023**, *175*, 107316. [CrossRef]
20. Hu, G.; Zhang, X.; Bu, M.; Lei, C. Toughening and strengthening epoxy resins with a new bi-DOPO biphenyl reactive flame retardant. *Eur. Polym. J.* **2022**, *178*, 111488. [CrossRef]
21. Zhang, J.; Duan, H.; Cao, J.; Zou, J.; Ma, H. A high-efficiency DOPO-based reactive flame retardant with bi-hydroxyl for low-flammability epoxy resin. *J. Appl. Polym. Sci.* **2020**, *138*, 50165. [CrossRef]

22. Li, Z.; Chen, M.; Li, S.; Fan, X.; Liu, C. Simultaneously improving the thermal, flame-retardant and mechanical properties of epoxy resins modified by a novel multi-element synergistic flame retardant. *Macromol. Mater. Eng.* **2019**, *304*, 1800619. [CrossRef]
23. Qi, Y.; Weng, Z.; Kou, Y.; Song, L.; Li, J.; Wang, J.; Zhang, S.; Liu, C.; Jian, X. Synthesize and introduce bio-based aromatic s-triazine in epoxy resin: Enabling extremely high thermal stability, mechanical properties, and flame retardancy to achieve high-performance sustainable polymers. *Chem. Eng. J.* **2021**, *406*, 126881. [CrossRef]
24. Bao, X.; Wu, F.; Wang, J. Thermal degradation behavior of epoxy resin containing modified carbon nanotubes. *Polymers* **2021**, *13*, 3332. [CrossRef] [PubMed]
25. Zhou, S.; Tao, R.; Dai, P.; Luo, Z.; He, M. Two-step fabrication of lignin-based flame retardant for enhancing the thermal and fire retardancy properties of epoxy resin composites. *Polym. Compos.* **2020**, *41*, 2025–2035. [CrossRef]
26. Gao, T.Y.; Wang, F.D.; Xu, Y.; Wei, C.X.; Zhu, S.E.; Yang, W.; Lu, H.D. Luteolin-based epoxy resin with exceptional heat resistance, mechanical and flame retardant properties. *Chem. Eng. J.* **2022**, *428*, 131173. [CrossRef]
27. Qian, X.; Song, L.; Bihe, Y.; Yu, B.; Shi, Y.; Hu, Y.; Yuen, R.K.K. Organic/inorganic flame retardants containing phosphorus, nitrogen and silicon: Preparation and their performance on the flame retardancy of epoxy resins as a novel intumescent flame retardant system. *Mater. Chem. Phys.* **2014**, *143*, 1243–1252. [CrossRef]
28. Zhi, M.; Yang, X.; Fan, R.; Yue, S.; Zheng, L.; Liu, Q.; He, Y. A comprehensive review of reactive flame-retardant epoxy resin: Fundamentals, recent developments, and perspectives. *Polym. Degrad. Stab.* **2022**, *201*, 109976. [CrossRef]
29. Mostovoy, A.S.; Yakovlev, A.V.; Lopukhova, M.I. Directional control of physico-chemical and mechanical properties of epoxide composites by the addition of graphite-graphene structures. *Polym. Plast. Technol. Mater.* **2019**, *59*, 874–883. [CrossRef]
30. Qi, Y.; Weng, Z.; Zhang, K.; Wang, J.; Zhang, S.; Liu, C.; Jian, X. Magnolol-based bio-epoxy resin with acceptable glass transition temperature, processability and flame retardancy. *Chem. Eng. J.* **2020**, *387*, 124115. [CrossRef]
31. Cui, M.; Li, J.; Chen, X.; Hong, W.; Chen, Y.; Xiang, J.; Yan, J.; Fan, H. A halogen-free, flame retardant, waterborne polyurethane coating based on the synergistic effect of phosphorus and silicon. *Prog. Org. Coat.* **2021**, *158*, 106359. [CrossRef]
32. Luo, H.; Rao, W.; Liu, Y.; Zhao, P.; Wang, L.; Yu, C. Novel multi-element DOPO derivative toward low-flammability epoxy resin. *J. Appl. Polym. Sci.* **2020**, *137*, 49427. [CrossRef]
33. Luo, C.; Nan, C.; Zuo, J.; Lin, F. Effect of sulfur in different valence on flame retardance of epoxy resin for light emitting diode. *J. Appl. Polym. Sci* **2020**, *138*, 50271. [CrossRef]
34. Liu, D.; Cui, Y.; Zhang, T.; Zhao, W.; Ji, P. Improving the flame retardancy and smoke suppression of epoxy resins by introducing of DOPO derivative functionalized ZIF-8. *Polym. Degrad. Stab.* **2021**, *194*, 109749. [CrossRef]
35. Liu, B.W.; Zhao, H.B.; Wang, Y.Z. Advanced flame-retardant methods for polymeric materials. *Adv. Mater.* **2022**, *34*, 2107905. [CrossRef]
36. Zhao, Z.; Wang, J.; Wang, J.; Chen, K.; Zhang, B.; Chen, Q.; Guo, P.; Wang, X.; Liu, F.; Huo, S.; et al. Facile fabrication of single-component flame-retardant epoxy resin with rapid curing capacity and satisfied thermal resistance. *React. Funct. Polym.* **2022**, *170*, 105103. [CrossRef]
37. Bifulco, A.; Varganici, C.D.; Rosu, L.; Mustata, F.; Rosu, D.; Gaan, S. Recent advances in flame retardant epoxy systems containing non-reactive DOPO based phosphorus additives. *Polym. Degrad. Stab.* **2022**, *200*, 109962. [CrossRef]
38. Zhang, Y.; Shi, C.; Qian, X.; Jing, J.; Jin, L. DOPO/Silicon/CNT nanohybrid flame retardants: Toward improving the fire safety of epoxy resins. *Polymers* **2022**, *14*, 565. [CrossRef]
39. Cao, M.; Liu, B.W.; Zhang, L.; Peng, Z.C.; Zhang, Y.Y.; Wang, H.; Zhao, H.B.; Wang, Y.Z. Fully biomass-based aerogels with ultrahigh mechanical modulus, enhanced flame retardancy, and great thermal insulation applications. *Compos. Part B* **2021**, *225*, 109309. [CrossRef]
40. Gong, K.; Yin, L.; Pan, H.; Mao, S.; Liu, L.; Zhou, K. Novel exploration of the flame retardant potential of bimetallic MXene in epoxy composites. *Compos. Part B* **2022**, *237*, 109862. [CrossRef]
41. Huo, S.; Zhou, Z.; Jiang, J.; Sai, T.; Ran, S.; Fang, Z.; Song, P.; Wang, H. Flame-retardant, transparent, mechanically-strong and tough epoxy resin enabled by high-efficiency multifunctional boron-based polyphosphonamide. *Chem. Eng. J.* **2022**, *427*, 131578. [CrossRef]
42. Luo, H.; Rao, W.; Zhao, P.; Wang, L.; Liu, Y.; Yu, C. An efficient organic/inorganic phosphorus-nitrogen-silicon flame retardant towards low-flammability epoxy resin. *Polym. Degrad. Stab.* **2020**, *178*, 109195. [CrossRef]
43. Yu, C.; Wu, T.; Yang, F.; Wang, H.; Rao, W.; Zhao, H.B. Interfacial engineering to construct P-loaded hollow nanohybrids for flame-retardant and high-performance epoxy resins. *J. Colloid Interface Sci.* **2022**, *628*, 851–863. [CrossRef] [PubMed]
44. Tao, J.; Yang, F.; Wu, T.; Shi, J.; Zhao, H.B.; Rao, W. Thermal insulation, flame retardancy, smoke suppression, and reinforcement of rigid polyurethane foam enabled by incorporating a P/Cu-hybrid silica aerogel. *Chem. Eng. J.* **2023**, *461*, 142061. [CrossRef]
45. Luo, Y.; Wang, S.; Du, X.; Du, Z.; Cheng, X.; Wang, H. Durable flame retardant and water repellent cotton fabric based on synergistic effect of ferrocene and DOPO. *Cellulose* **2021**, *28*, 1809–1826. [CrossRef]
46. Zhang, W.; Fina, A.; Ferraro, G.; Yang, R. FTIR and GCMS analysis of epoxy resin decomposition products feeding the flame during UL 94 standard flammability test. Application to the understanding of the blowing-out effect in epoxy/polyhedral silsesquioxane formulations. *J. Anal. Appl. Pyrolysis* **2018**, *135*, 271–280. [CrossRef]
47. Wang, X.; He, W.; Long, L.; Huang, S.; Qin, S.; Xu, G. A phosphorus and nitrogen-containing DOPO derivative as flame retardant for polylactic acid (PLA). *J. Therm. Anal. Calorim.* **2020**, *145*, 331–343. [CrossRef]

48. Zhao, P.; Rao, W.; Luo, H.; Wang, L.; Liu, Y.; Yu, C. Novel organophosphorus compound with amine groups towards self-extinguishing epoxy resins at low loading. *Mater. Des.* **2020**, *193*, 108838. [CrossRef]
49. Yu, C.; Wu, T.; Yang, F.; Rao, W.; Zhao, H.-B.; Zhu, Z. Construction of hetero-structured nanohybrid relying on reactive phosphazene towards flame retardation and mechanical enhancement of epoxy resins. *Eur. Polym. J.* **2022**, *167*, 111075. [CrossRef]